

Microwave excited optical transparency enhancement resonances in Hanle-EIT configuration

Yisheng Ma (马易升), Jianliao Deng (邓见辽), Zhengfeng Hu (胡正峰),
Huijuan He (何慧娟), and Yuzhu Wang (王育竹)*

Key Laboratory for Quantum Optics, Center for Cold Atom Physics, Shanghai Institute of Optics and Fine Mechanics,
Chinese Academy of Sciences, Shanghai 201800, China

*Corresponding author: yzwang@mail.shcnc.ac.cn

Received May 25, 2012; accepted October 10, 2012; posted online January 21, 2013

We report an experimental observation of the optical transparency enhancement resonances in Hanle-electromagnetically induced transparency (EIT) configuration with a microwave field excitation. In this experimental system, a strong control field and a weak probe field form three-level Λ -type configurations of EIT. The fourth level is coupled by an additional microwave field. With the microwave field excitation, the probe field undergoes a process of absorption to transparency when the probe field decreases. Compared with the EIT effect, this result indicates optical transparency enhancement. A simple theoretical model and a numerical simulation are presented to explain the observed experimental results. The applications of these optical features are also discussed.

OCIS codes: 270.1670, 190.4180.
doi: 10.3788/COL201311.022701.

Since the phenomenon of electromagnetically induced transparency (EIT) has been observed, it has attracted great attention among researchers in the fields of nonlinear and quantum optics as well as in spectroscopy and precision metrology^[1,2]. EIT refers to a phenomenon, in which a probe field experiences reduced absorption at the center of the probe transition in an absorbing medium driven by a control field. The essential feature of EIT is the existence of quantum superposition states, which are decoupled from the coherent and dissipative interactions^[3]. As a general rule, interactions involving such a “dark state” may lead to a modification of the atomic-optical responses^[4]. The interactions can come from different sources: a microwave^[5], optical coherent^[6–8], direct current or alternating current^[9], or radio frequency fields^[10]. The observed results show various phenomena, such as absorption, transparency, and optical gain. Optical properties, such as width, amplitude, and position, can be manipulated by adjusting the coherent interaction.

In this letter, we demonstrate the observation of optical transparency enhancement resonances in a rubidium (⁸⁷Rb) vapor cell. In this experimental system, a strong control field and a weak probe field formed several three-level Λ -type configurations of EIT. A microwave field drove a magnetic-dipole transition between the fourth level and ground state, which is coupled with the excited state by the control field. The probe light undergoes a process of absorption to transparency when the probe field decreases step by step. To our knowledge, this observation has not been reported previously; moreover some new interesting applications, such as sensitive spectroscopy, can be carried out using these effects.

To realize Hanle-EIT configuration, the relevant energy levels and excitation laser and microwave fields are shown in Fig. 1(a). The control field (Rabi frequency Ω_c) and the probe field (Rabi frequency Ω_p) are represented by right and left circularly polarized light (σ^+ and σ^-), respectively, as derived from a single linear

polarized laser beam. These light fields coupled pairs of Zeeman sublevels of ground state ($5^2S_{1/2}$) ⁸⁷Rb atoms with magnetic quantum numbers differ by two through the excited $5^2P_{1/2}$, $F = 2$ state. Given that the ground-state sublevels have the same energies, the Hanle-EIT and related coherent effects can be observed around the zero magnetic field^[11]. In this case, an additional microwave field coupled the fourth state $5^2S_{1/2}$, $F = 1$, $m_F = 0$ to $5^2S_{1/2}$, $F = 2$, $M_F = 0$. In this experiment, the control field is much stronger than the probe field ($\Omega_c \gg \Omega_p$), and most of the relevant atoms are pumped in the state $5^2S_{1/2}$, $F = 2$, $M_F = 2$ and in the other three ground states ($5^2S_{1/2}$, $F = 1$, $M_F = 0, \pm 1$). Thus, we can focus on the realistic systems shown as |a>, |b>, |c>, and |d>, respectively. The reservoir of spectator states can thus be collectively marked as |e>, which is

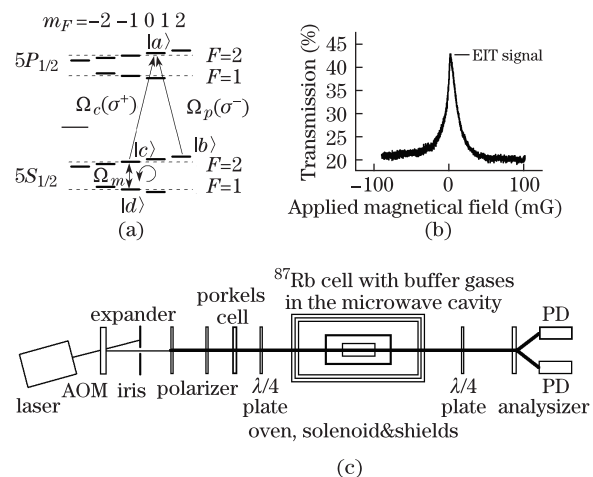


Fig. 1. (a) Four-level configuration of ⁸⁷Rb atomic states resonantly coupled to a control field (Ω_c), a probe field (Ω_p), and a microwave field (Ω_m); (b) typical observed ⁸⁷Rb EIT, in which the transmission intensity is shown as a function of the magnetic field, the full width of the resonance is about 20 mG; (c) schematic of the experimental setup.

calculated in the numerical simulation.

We performed the experiments in warm pure ^{87}Rb vapor with mixture buffer gases Ar (15.5 Torr) and N_2 (9.5 Torr) heated to 62 °C to obtain around 80% resonant absorption for a weak optical field of the ^{87}Rb D_1 line ($\cong 795$ nm). The experimental setup is shown in Fig. 1(c). The ^{87}Rb cell was placed inside a TE_{011} microwave cavity for the microwave field excitations, and a cylindrical coil surrounded the cavity for the magnetic field control. The coil and cell were placed inside a three-layer cylindrical μ -metal shield to render the remnant magnetic field to less than 20 μG . The laser frequency was stabilized by employing the saturated absorption spectroscopy technique. An acousto-optical modulator (AOM) shifted the light frequency 160 MHz corresponding to the buffer gas mixture frequency shift of the input light, and was also used as an intensity controller of the light. The input laser beam was collimated and expanded into a diameter of 8 mm and then passed through the sample cell. For the data presented here, we employed the $5^2S_{1/2}, F = 2 \rightarrow 5^2P_{1/2}, F = 2$ transition of ^{87}Rb . The laser beam was divided into control and probe beams with a fast Pockels cell and two $\lambda/4$ plates. We slightly rotated the polarization of the input light to generate a weak left circular polarized probe light (σ^-) and a strong right circular polarized control light (σ^+). The 6.8-GHz microwave field was applied to drive the magnetic-dipole transition between $|F = 1\rangle$ and $|F = 2\rangle$. The probe and control lights were separated by a high-quality polarizer and analyzer with an extinction ratio of 1×10^{-5} ; these were detected using individual photo detectors, and then recorded in the oscilloscope. We firstly considered the case of the continuous wave (CW) probe and control fields. Figure 1(b) displays a typical transmission spectrum for the probe (Ω_p) field obtained by scanning the magnetic field. Due to the induced transparency, the probe field transmission was maximal for zero magnetic field, despite the fact that most atoms are in the state $5^2S_{1/2}, F = 2, m_F = 2$ for the three-level Λ -type configuration. We set the control field to 1 mW and the probe field to 50 μW ; Given that some atoms were out of the three-level system, the observed EIT was not perfect with the contrast of around 24%. Outside of the transparency window (magnetic field 20 mG), the Rb vapor can be deemed nearly opaque to the probe field.

We next applied a microwave field to drive the magnetic-dipole transition between $|F=1\rangle$ and $|F=2\rangle$. We applied a 32 mG static magnetic field to separate the hyperfine zeeman sublevels. Firstly, we set the control field to 1 mW, the probe field to 50 μW , and the microwave field output power to 16 dBm. We detected the transmission intensity of the probe field and the experimental observation is shown in Fig. 2. The base line we define here is the peak value of transparent resonance (Fig. 1(b)), when the microwave field is turned far away from the resonance. In this case, the microwave field has no direct influence on the EIT effects. When we scanned the frequency of the microwave field near the hyperfine transitions of the ground states, seven deep absorption peaks appeared (Fig. 2(a)). These peaks correspond to the nine microwave magnetic-dipole transitions, two of which are degenerate. Next we carefully rotated the pockels cell to decrease the probe light to around

1 μW . We found that the seven absorption peaks gradually reduced and then turned to optical transparency (Fig. 2(b)). Compared with the base line, we obtain the optical transparency enhancement resonances. The signal-to-noise ratio (SNR) of the highest peak is far greater than 160 for a 100-kHz bandwidth of the detection system. The observed optical transparency strongly related to the ratio of the intensity of probe light and control light (Fig. 2(c)), and the linewidth and contrast of the peaks depended mainly on the microwave field output power (Fig. 2(d)). The distance between the peaks is the split by the Zeeman interaction. Compared with the optical absorptive resonance and EIT, the optical transparent resonance had higher contrast, narrower linewidth. We focused on the central peak, corresponding to the magnetic-dipole transition $5^2S_{1/2}, F = 1, m_F = 0 \rightarrow 5^2S_{1/2}, F = 2, m_F = 0$. As the magnetic quantum number ($m_F = 0$) equals zero, the peak had no first-order magnetic field effect. The width of the peak became narrower to sub-kHz when the microwave field output power was reduced. The contrast which is defined as (maximum-minimum)/maximum could reach up to 25%.

In order to analyze the experimental data and compare it with the theoretical explanation, we calculated the probe field spectra by solving the optical Bloch equation of density-matrix operator described as

$$\frac{d\rho}{dt} = \frac{1}{i\hbar}(H_{\text{atom}} + H_{\text{coupling}} + H_{\text{microwave}} + H_{\text{probe}}, \rho) + \left\{ \frac{d\rho}{dt} \right\}, \quad (1)$$

where H_{atom} is the atom Hamiltonian; H_{coupling} , $H_{\text{microwave}}$, and H_{probe} are the Hamiltonian of the coupling, microwave, and probe fields in the rotating-wave approximation, respectively. $\left\{ \frac{d\rho}{dt} \right\}$ describes the relaxation of ρ and its elements as

$$\left\{ \frac{d\rho_{aa}}{dt} \right\} = -(\Gamma_b + \Gamma_c + \Gamma_d + \Gamma_e)\rho_{aa}, \quad (2)$$

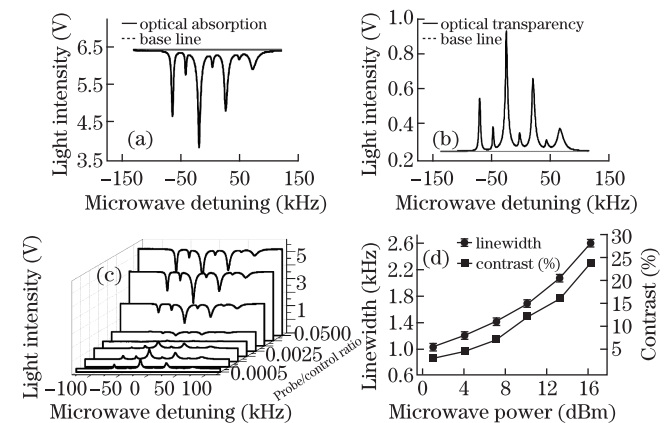


Fig. 2. Parallel static magnetic field is applied, the peaks are split into seven peaks, and the distance between the adjacent peaks or the zeeman frequency shift is at 22.5 kHz, $I_c = 1$ mW. (a) Optical absorption, $I_p = 50$ μW ; (b) optical transparency, $I_p = 1$ μW ; (c) optical response as a function of the probe-to-control intensity ratio; (d) linewidth and contrast of the central peak as a function of the microwave output power.

$$\left\{ \frac{d\rho_{bb}}{dt} \right\} = \Gamma_b \rho_{aa} + \gamma_1(\rho_{cc} - \rho_{bb}) + \gamma_1(\rho_{dd} - \rho_{bb}) + \gamma_1(\rho_{ee} - 2\rho_{bb}), \quad (3)$$

$$\left\{ \frac{d\rho_{cc}}{dt} \right\} = \Gamma_c \rho_{aa} + \gamma_1(\rho_{bb} - \rho_{cc}) + \gamma_1(\rho_{dd} - \rho_{cc}) + \gamma_1(\rho_{ee} - 2\rho_{cc}), \quad (4)$$

$$\left\{ \frac{d\rho_{dd}}{dt} \right\} = \Gamma_d \rho_{aa} + \gamma_1(\rho_{bb} - \rho_{dd}) + \gamma_1(\rho_{cc} - \rho_{dd}) + \gamma_1(\rho_{ee} - 2\rho_{dd}), \quad (5)$$

$$\left\{ \frac{d\rho_{ee}}{dt} \right\} = \Gamma_e \rho_{aa} + \gamma_1(2\rho_{bb} - \rho_{ee}) + \gamma_1(2\rho_{cc} - \rho_{ee}) + \gamma_1(2\rho_{dd} - \rho_{ee}), \quad (6)$$

$$\left\{ \frac{d\rho_{ij}}{dt} \right\} = -\Gamma_{ij} \rho_{ij}, \quad (i, j = a, b, c, d), \quad (7)$$

with

$$\Gamma_{ab} = \frac{\Gamma_b}{2}, \quad \Gamma_{ac} = \frac{\Gamma_c}{2}, \quad \Gamma_{ad} = \frac{\Gamma_d}{2}, \\ \Gamma_{bc} = \Gamma_{bd} = \Gamma_{cd} = \gamma_0, \quad (8)$$

where Γ_b , Γ_c , Γ_d , and Γ_e are the spontaneous decay rates from $|a\rangle$ to $|b\rangle$, $|c\rangle$, $|d\rangle$, and $|e\rangle$, respectively; γ_1 represents the atoms and buffer gases collisions induced decay rate; γ_0 represents the relaxation rate of coherence between the ground states. The probe properties is proportional to the imaginary part of the amplitude of ρ_{ab} in the units η , $\eta = \mathcal{N}\lambda^3/(8\pi^2)$, in which \mathcal{N} is the atomic density, and λ is the light field wavelength. We took our numerical simulation parameters from our experimental measurement and some parameters of the cell from Ref. [13]. The results are consistent with our observation and are shown in Fig. 3.

We turn to an interpretation of the experimental results. The coherence $\text{Im}(\rho_{ab})$ in the steady state can be written as

$$\text{Im}[\rho_{ab}(\Delta_m)] = -\frac{\Omega_p[\rho_{bb}(\Delta_m) - \rho_{aa}(\Delta_m)] + \Omega_c \text{Re}[\rho_{bc}(\Delta_m)]}{\Gamma_{ab}}. \quad (9)$$

The probe response is attributed to two terms, namely, the population difference $\rho_{bb} - \rho_{aa}$ and the atomic coherence $\text{Re}(\rho_{bc})$ multiplied by the Rabi frequencies of the

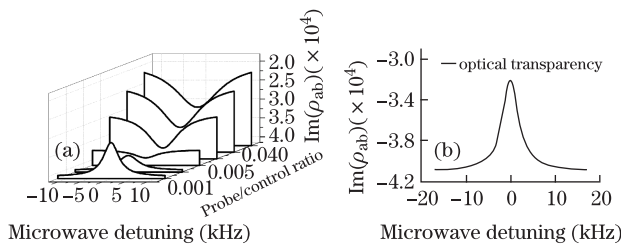


Fig. 3. Imaginary part of the susceptibility in the units η , the parameters are $\Gamma_b = \Gamma_c = \Gamma_d = 1.3 \times 10^6 \text{ s}^{-1}$, $\Gamma_e = 2.6 \times 10^6 \text{ s}^{-1}$, $\gamma_1 = 282 \text{ s}^{-1}$, $\gamma_0 = 290 \text{ s}^{-1}$, $\Omega_c = 6.8 \times 10^6 \text{ s}^{-1}$, and $\Omega_m = 3400 \text{ s}^{-1}$. (a) Optical response as a function of the probe-to-control intensity ratio; (b) optical transparency when $\Omega_p = 2.7 \times 10^5 \text{ s}^{-1}$.

probe and control lights, respectively. In the absence of microwave excitation, which is the condition for EIT, the first term has almost the same value as the second term, assuming that the control light is strong enough to approximate $\rho_{bb} - \rho_{aa} = 1$ and that the dephasing factors, such as Γ_{bc} can be ignored^[2]. Following the theoretical predictions discussed in Ref. [4], it can be made to optical gain in the presence of microwave field. However, the realistic system is not perfect (Fig. 1(b)). It can be separated into two cases to qualitatively understand our experimental system. The two terms do not cancel perfectly because of the microwave excitation and have a competitive relation with the microwave detuning. Normally, the spectrum shows optical absorption resonance due to the population loss and the destruction of the coherence^[4,5]. However, it shows a different view when the probe field is weaker. Some atoms are incoherently injected into $|d\rangle$ from the other states due to collisions between the buffer gases and atoms^[12], which leads to the situation wherein the variation of the first term is greater than that of the second term. In the four-level dressed picture^[4], the three-photon transition from $|d\rangle$ to $|b\rangle$ resulted in an increase in the imaginary part of the susceptibility ($\text{Im}(\rho_{ab})$) at the transparency point, which reduced the absorption of the probe field.

Our results show that there are some possible applications for high-resolution laser spectrum, EIT-based atomic clock. These clocks can provide a sensitive tool for direct measurements of the strength of the coherent perturbation such as microwave field, among others. High sensitivity similar to EIT-based techniques can be expected, but without the need for involved dispersive measurements since narrow optical resonances can be observed with a large SNR. After checking the central peak in the several peaks spectrum. The peak cancelled the first-order magnetic effect, which is a good reference for the atomic frequency standard.

In conclusion, we show an experimental observation of the optical transparency enhancement resonances in Hanle-EIT configuration. With the microwave field excitation, the probe light field turns from absorption to optical transparency when the probe field decreases. The theoretical model and numerical simulation illustrate that some atoms are injected into the foul-level system which lead to optical transparency enhancement resonance. Due to the large SNR, the resonances can be applied to high-resolution spectroscopy, EIT based atomic clock.

We thank Jinda Lin for his useful help. This work was supported by the Major State Basic Research Development Program of China under Grant No. 2005CB724507.

References

1. S. E. Harris, Phys. Today **50**, 36 (1997).
2. M. Fleischhauer, A. Imamoglu, and J. P. Marangos, Rev. Mod. Phys. **77**, 633 (2005).
3. S. E. Harris, J. E. Field, and A. Imamoglu, Phys. Rev. Lett. **64**, 1107 (1990).
4. M. D. Lukin, S. F. Yelin, M. Fleischhauer, and M. O. Scully, Phys. Rev. A **60**, 3225 (1999).
5. Y.-C. Chen, Y.-A. Liao, H.-Y. Chiu, J.-J. Su, and I. A. Yu, Phys. Rev. A **64**, 053806 (2001).

6. C. Champenois, G. Morigi, and J. Eschner, *Phys. Rev. A* **74**, 053404 (2006).
7. Z. Wang and Y. Tang, *Chin. Opt. Lett.* **6**, 405 (2010).
8. M. Yan, E. G. Rickey, and Y. Zhu, *Opt. Lett.* **26**, 548 (2001).
9. E. A. Wilson, N. B. Manson, and C. Wei, *Phys. Rev. A* **72**, 063814 (2005).
10. S. F. Yelin, V. A. Sautenkov, M. M. Kash, G. R. Welch, and M. D. Lukin, *Phys. Rev. A* **68**, 063801 (2003).
11. W. Hanle, *Z. Phys.* **30**, 93 (1924).
12. M. A. Bouchiat, J. Brosset, and L. C. Pottier, *J. Chem. Phys.* **56**, 3703 (1972).
13. S. Micalizio, A. Godone, F. Levi, and C. Calosso, *Phys. Rev. A* **79**, 013403 (2009).